Chapter 5
Weather Prediction Models

Julio T. Bacmeister

Glossary

Assimilation	The process of combining observations of the atmosphere with a "first guess" (usually a model forecast) to define the atmospheric state on a forecast model grid.
Geostrophic balance	A possible state of rotating fluids in which flow is directed along pressure gradients rather than across them.
Gravity waves	Rapidly moving atmospheric disturbances driven by gravity acting on vertical density gradients. Often arise as a consequence of spurious geostrophic imbalance in initial conditions.
Hydrostatic balance	State in which the vertical pressure gradient force cancels the downward accleration of gravity. Approximately obeyed in atmospheric flows with horizontal scales larger than several km.
Instabilities (or unstable modes)	Spatial patterns in a flow that are able to extract energy from the background flow and grow in amplitude.
Primitive equations	Complete set of equations describing flow of a thin envelope of fluid or gas surrounding a sphere.
Resolution	Separation in space of notional points at which quantities are defined in a numerical model.

This chapter was originally published as part of the Encyclopedia of Sustainability Science and Technology edited by Robert A. Meyers. DOI:10.1007/978-1-4419-0851-3

J.T. Bacmeister (✉)
NCAR Earth System Laboratory, National Center for Atmospheric Research,
1850 Table Mesa Drive, 80305 Boulder, CO, USA
e-mail: juliob@ucar.edu

P.J. Rasch (ed.), *Climate Change Modeling Methodology: Selected Entries from the Encyclopedia of Sustainability Science and Technology*,
DOI 10.1007/978-1-4614-5767-1_5,

Definition of the Problem

Awareness of weather and concern about weather in the proximate future certainly must have accompanied the emergence of human self-consciousness. Although weather is a basic idea in human existence, it is difficult to define precisely. Weather intuitively refers to a set of atmospheric conditions prevailing over a relatively small area, and even more emphatically, over a relatively short time. The immediacy contained in our notion of weather may be reflected in the fact that in many languages the same root appears in the words for time and weather, for example, Spanish (*tiempo*) or Hungarian (*idö*). Thus, weather is to be distinguished from the notion of climate, or more subtly from the notion of "spells" which imply a time window anywhere from a week to several years. Our experience of weather does involve quantities which can be defined with reasonable precision. These include air temperature, wind speed, precipitation rates and types, cloud cover, and also humidity, air-quality, and barometric pressure. Numerical weather prediction (NWP) is the attempt to predict the evolution of such quantities by solving a set of partial differential equations which describe the dynamics of a fluid like the atmosphere [1, 2]. These equations must be solved using approximate or "numerical" techniques using computers. They are integrated forward in time from a set of initial conditions, which are derived from an optimized combination of observations and previous model forecasts. This bootstrapped procedure is known as the analysis cycle and is an integral part of the activities at all modern forecasting centers.

NWP and global climate simulation are closely related problems. The models used in both endeavors are essentially the same. A key difference between NWP and the climate problem is the role of atmospheric initial conditions. Initialization of the atmosphere is of secondary importance in multiyear climate simulations. However, good initialization of the atmospheric state is at the heart of the forecasting problem. Initialization must give an accurate and comprehensive representation of the state of the atmosphere that is compatible with numerical forecast model being used. The initial state must also satisfy a number of "balance constraints" to avoid spurious initial variability.

Lewis Fry Richardson (1881–1953) reported the first numerical weather forecast, performed using hand calculations, in 1922 [3]. His attempt did not succeed for reasons that are summarized below, and discussed in detail in the book by Lynch [2], but Richardson's effort marks the beginning of NWP as a field of inquiry.

Introduction: Direct Simulation of Atmospheric Flows

In order to appreciate the challenges faced by numerical models of the global atmosphere it is useful to have a sense of the complex nature of the motions which must be represented. A brief account of some of the dynamical processes

Table 5.1 Motions in atmosphere

Phenomenon	Spatial scale	Temporal scale	Role in weather
Acoustic waves	Meters	Seconds	None
Gravity waves	1–1,000 km	15 min to days	Initiating and organizing convection. Mountain flows, e.g., chinooks, Foehns . . .
Eastery waves	500–2,000 km	Days	Organizing tropical convection, tropical cyclogenesis
Baroclinic instability	Thousands of km	Days	Midlatitude cyclogenesis
Madden–Julian oscillation	10,000 km	20–60 days	Possible modulation of tropical and midlatitude weather

that play a part in weather is given below. For more details, the reader is referred to the excellent, comprehensive introduction to the dynamics of the atmosphere and ocean by A.E. Gill (1937–1986) [4].

A Zoology of Atmospheric Motion

The atmospheric flows which are responsible for creating weather span a wide range of space and time scales and are driven by rich variety of dynamical and thermodynamic processes. Atmospheric flows may be forced by features at the Earth's surface. Mountainous terrain forces atmospheric circulations with spatial scales ranging from several kilometers to several thousand kilometers. Surface temperature contrasts, most pronounced between land and ocean but also created by variations in ground cover, force sea-breeze circulations with scales of tens of kilometers, [5] as well as continental-scale monsoonal circulations (Table 5.1) [6–8].

External forcing can produce wave-like motions in the atmosphere. Gravity waves, or buoyancy waves, exist because of density stratification in the atmosphere, and are analogs to waves on the surface of water. These waves are typically one to hundreds of kilometers in scale, and have periods of minutes to hours, although in the tropics both spatial and temporal scales may be longer [4]. Gravity waves may play a role in triggering convection [9–11], as well as in organizing convection in the mesoscale [10, 12, 13]. Mountain waves are large, nonlinear, gravity waves generated by flow over mountains with horizontal scales from less than ten kilometers to several hundred kilometers. Such waves are responsible for a number of local but intense winds [14]. Gravity waves are also notorious for contaminating forecasts when errors in initial conditions are present.

Rossby waves [4, 15–17] named after the Swedish meteorologist Carl Gustav Rossby exist because of the change in the effective rotation rate experienced by a fluid parcel as it moves from equator to pole. The effective rotation rate at the

Equator is zero, since all of the effects of Earth's rotation are directed in the vertical and are felt as a slight reduction in the pull of gravity. At the poles, the effective rotation rate is as intuitively expected – one cycle or 2π radians per day. In between equator and pole, this rate varies as the sine of latitude. Rossby waves which exploit this gradient have scales of thousands to ten thousands of kilometers and periods of days to weeks. Immense planetary-scale Rossby waves or "planetary waves" generated by topographic features such as the Himalayas and Rockies, as well as, by continental-scale land-sea contrasts, dominate the tropospheric flow and are responsible for the mean position of the jet-streams, and for the mean paths of storms.

Probably more important in the overall problem of weather, and certainly more difficult to predict, is another class of flows driven by internal exchanges of energy in the atmosphere. These instabilities or unstable modes are essentially flow patterns that are able to extract energy from their surroundings and grow in amplitude. Initial growth of unstable modes is typically exponential. Familiar examples of such behavior in fluids include the growth of wind driven waves on the surface of water. The convective instability of a fluid heated from below is another example that is both familiar in everyday experience and also important in the atmosphere.

In the atmosphere, a particularly important mode of unstable growth is through baroclinic instability [18, 19]. This instability arises from a combination of thermal and inertial effects in a rotating fluid with a horizontal temperature along the lower boundary. Baroclinic instability is characterized by length scales of 1,000 km and growth times of days – making it a key factor in weather. It is fair to say that the problem of weather forecasting in midlatitudes is essentially that of predicting the evolution of baroclinically unstable modes in the atmosphere.

The tropics possess another as yet poorly understood class of motions, in which moist heating plays a key role in energizing and modifying wave motions in the atmosphere [20]. Tropical easterly waves [21] have periods of several days and scales of hundreds to thousands of kilometers and play an important role in the genesis of tropical cyclones [22–24]. The Madden–Julian oscillation or "MJO" [25, 26] is an eastward traveling disturbance in the tropics with a length scale close to 10,000 km and a period of weeks. It is thought to play a role in modulating tropical cyclone frequency in various basins [27–31] and possibly midlatitude disturbances as well [32, 33]. The dynamics behind the MJO are not yet understood. Successful forecasting of the MJO could improve prospects for accurate forecasts out to lead times of weeks [34].

Early History

Weather prediction, not climate simulation, was the original motivation for developing numerical models that describe the time evolution of the atmosphere. Richardson's 1922 attempt at NWP predates initial attempts to study climate

numerical models by at least four decades. The first attempts at simulating the longer-term equilibrium state of the atmosphere did not occur until the 1960s [35].

The notion of predicting weather systematically using equations to describe the evolution of systems can probably be traced to the Norwegian meteorologist Vilhelm Bjerknes (1862–1951) [1, 2] who founded the famous "Bergen School" of meteorology [36, 37]. Bjerknes considered graphical methods to predict the motion of fronts and other features in the atmosphere, as well as numerical techniques to solve the equations themselves. However, it was L. F. Richardson who finally conceived and implemented a concrete plan to use a numerical solution of the partial differential equations describing the atmosphere (see section on "primitive equations") to make forecasts. His approach was remarkably prescient both in concept and in detail. He employed a finite-difference technique on a regularly spaced grid of points over central Europe and attempted to predict the tendency of surface pressure over 6 h. Richardson's forecast was a famous failure or "bust" (see the book by Lynch [2] for a detailed and readable account of Richardson's attempt, as well as for a comprehensive account of the development of NWP). However, the reasons for Richardson's failure lay in the initial conditions used in the forecast not in his method as Richardson himself suspected [2].

The potential for numerical prediction was clear. The major obstacle beside the question of initialization, was the sheer amount of calculation required to produce even a short forecast over a limited area. Richardson imagined computational "factories" employing thousands of people to produce weather forecasts [2]. The appearance of electronic computers soon after World War II made numerical prediction plausible. The potential application to the problem of weather prediction was recognized by one of the main intellects behind the development of electronic computers John von Neumann (1903–1957) [1]. In the first successful attempts at NWP using electronic computers so-called filtered equation sets were used [2]. Filtered equations describe a limited set of atmospheric motions, but allow large time steps to be taken in numerical integration and side step the need for well-balanced initial conditions (see sections on "Numerics and Initialization").

Development of Modern NWP Models

It was recognized early on by Jule Charney and others that models using filtered equations were not a promising long-term path for NWP [2]. As computer power increased, the limitations on the time-step length allowed by more complete equations became less important. The problem of initialization was not solved, but its tractability became apparent [38]. Development work on NWP models using the primitive equations began in the late 1950s and eventually led to the adoption of primitive equation models at all major forecasting centers by the mid 1960s [2].

The Primitive Equations

The primitive equations are essentially the complete Navier–Stokes or Euler equations for fluid motion with the hydrostatic approximation invoked. As long as the horizontal scales of interest are much larger than 10 km, the hydrostatic approximation is well satisfied. However, at the time of writing, major NWP models are reaching horizontal resolutions that test the limits of this approximation. The Euler equations using a generalized vertical coordinate η, including connections between the fully nonhydrostatic system and the hydrostatic system currently used in NWP models, are nicely described by Laprise [39].

The hydrostatic primitive equations include an equation describing the evolution of horizontal momentum or velocity V:

$$\frac{d}{dt}V + f\mathrm{k} \times V = -\alpha\nabla_\eta p - \nabla_\eta \phi + F_{phys}$$

where f is the Coriolis parameter or local apparent rotation rate and k is the unit vector in vertical direction. The symbol ∇_η denotes a gradient along surfaces of fixed η. As is common in the meteorological literature φ denotes the geopotential height or potential energy density of a fluid parcel along constant η. The remaining symbols α and p denote specific volume and pressure. This equation is simply the fluid dynamical form of Newton's law $F = ma$, where the right-hand side contains forces accelerating fluid parcels in the horizontal. In current meteorological literature, the individual velocity components are usually designated as u for the eastward or "zonal" component, and v for the northward or "merdional" component.

Another equation restates the first law of thermodynamics $dE = dQ + dW$ in fluid form:

$$C_p \frac{d}{dt}T - \alpha \frac{d}{dt}p = H_{phys}$$

where T is the absolute temperature and C_p is the heat capacity of air at constant pressure. In both the momentum and energy equations the symbol $\frac{d}{dt}$ is used to denote:

$$\left(\frac{\partial}{\partial t}\right)_\eta + V \cdot \nabla_\eta + \dot{\eta}\frac{\partial}{\partial \eta}$$

the Lagrangian derivative that tracks changes in a quantity following a fluid parcel.

A prognostic equation for mass continuity is also required:

$$\left[\frac{\partial}{\partial t}\left(\frac{\partial p}{\partial \eta}\right)\right]_\eta + \nabla_\eta \cdot \left(V\frac{\partial p}{\partial \eta}\right) + \frac{\partial}{\partial \eta}\left(\dot{\eta}\frac{\partial p}{\partial \eta}\right) = 0$$

where $g^{-1}\frac{\partial p}{\partial \eta}$ is the mass per unit area in a column between surfaces of constant η.

Three diagnostic relationships are needed to complete the system. The equation of state for a gas:

$$p\alpha = RT$$

and a relationship that determines the geopotential height of η-surfaces:

$$\phi = \phi_s + \int_{\eta}^{\eta_s} \alpha \frac{\partial p}{\partial \eta'}\, d\eta$$

This relationship uses the surface geopotential height φ_s as well as the integral of the hydrostatic relationship:

$$\frac{\partial p}{\partial \eta} = \frac{1}{\alpha}\frac{\partial \phi}{\partial \eta}$$

between pressure and specific volume.

The right-hand sides of the momentum and energy equations also contain the terms F_{phys} and H_{phys}. These represent the effects of physical parameterizations on the grid scale variables, and include effects from radiative heating, friction, and other processes which will be described in more detail in the section on parameterization. The use of the generalized vertical coordinate η gives the equations a somewhat unfamiliar look. However, replacing η with the geometric height z, and noting that $\nabla_z \varphi = 0$ reduces them to a more familiar form.

Due to the complex shape of Earth's topography most NWP models do not use geometric height as their vertical coordinate. Most use a version of the so-called σ-coordinate defined by:

$$\sigma = \frac{p - p_t}{p_s(x, y, t) - p_t}$$

where $p_s(x, y, t)$ is the surface pressure and p_t is the pressure at the model top, typically a constant value. The coordinate surface $\sigma = 1$ follows the bottom of the model domain while $\sigma = 0$ follows the top. Boundary conditions on "vertical" velocity become simply $\dot{\sigma}(1) = \dot{\sigma}(0) = 0$. Thus, the difficulties of representing flow boundaries in and around topographic obstacles are replaced by the need for a prognostic equation describing π_s. This is obtained by integrating the mass continuity equation in the vertical.

The primitive equations can describe all of the motions discussed in the introduction except for fully three dimensional acoustic waves. They do allow a horizontal acoustic mode known as the Lamb wave [4] which can produce difficulties for numerical integrations. Gravity waves and convective instabilities with horizontal scales much smaller than 100 km are not well represented, and this

may become a significant handicap for models in the next 10 years (see section on "Future Directions").

In addition to the equations describing the dynamics and thermodynamics of the atmosphere, modern NWP models include equations that describe the evolution of trace gases and trace species in the atmosphere. Each additional species results in an additional prognostic equation of the form:

$$\frac{d}{dt} q_i = C_{i,phys}$$

where q_i is the mixing ratio of the ith species and $C_{i,phys}$ are the sources and losses of the species. The most important of these trace quantities is water vapor. Water vapor was included in primitive equation NWP models early on [40]. As NWP model domains were extended into the tropics during the 1970s [41] strong condensational heating associated with high tropical humidities presented problems for NWP that spurred the development of deep convection parameterizations [42] (see section on "Parameterization"). More recently, NWP models have incorporated prognostic treatment of condensed water species known as prognostic cloud schemes [43, 44].

Numerics

Closed form solutions of the primitive equations do not exist. Approximate numerical techniques must be used. An illustration of how this proceeds is given here using a simple equation that describes one dimensional advection of a constituent C by a constant flow u:

$$\partial_t C + u\partial_x C = S$$

Figure 5.1 shows three time steps from a numerical integration of this equation. Finite-difference approximations of the partial derivatives in both space and time are calculated as shown in the figure. The approach illustrated is known as a "centered difference" since the approximation uses a symmetric stencil of equally weighted points. With these approximations to the derivatives in time and space, a solution for the tracer distribution at $\tau + 1$ can be obtained:

$$C(i, \tau + 1) \approx C(i, \tau - 1) - u2\Delta t \left(\frac{C(i+1, \tau) - C(i-1, \tau)}{2\Delta x} \right)$$

As a technical detail, notice that to start (or initialize) this calculation two time levels of data must be given. In practice, these can be set equal to each other.

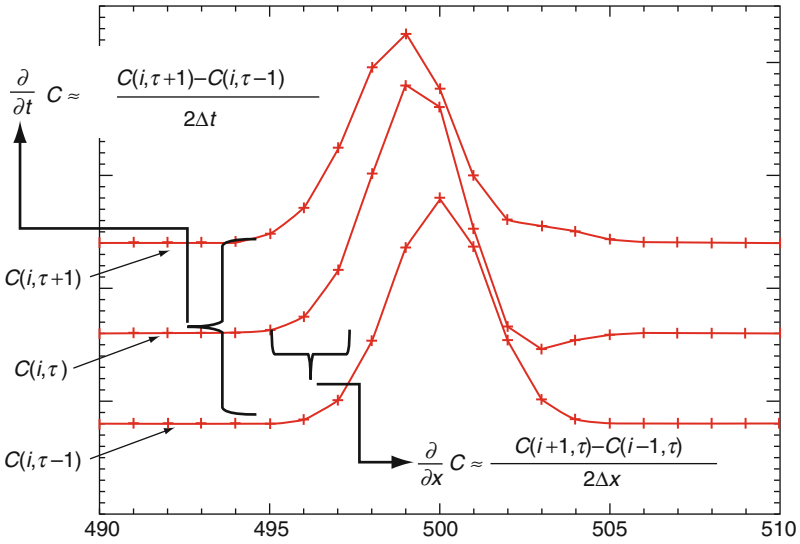

Fig. 5.1 Three time steps from numerical advection of a Gaussian tracer pulse using a second-order, space-centered, time-centered finite-difference scheme. The +'s indicate grid-point locations. A constant velocity of $u = -0.5$ is used with grid spacing $\Delta x = 1$ and time step $\Delta t = 1$

Once initial values are given, the arithmetic equation above can be repeated, or iterated, many times to give the time evolution of C.

The algorithm described above is a simple but stable scheme that was employed in early numerical models. However, it has many undesirable properties, which are described in [45]. Nevertheless, the basic concepts illustrated by this method hold for all explicit finite-difference approaches. In implicit methods, the terms in the approximation of $\partial_x C$ above are replaced by their values at time $\tau + 1$. In the case above, this leads to a tridiagonal matrix problem that can be easily solved using standard techniques [45].

The most natural coordinate system for a global atmospheric model is spherical, with latitude and longitude as the horizontal coordinates. Unfortunately, as either pole is approached, equally spaced longitude lines come arbitrarily close together. This presents problems for most finite-difference numerical schemes, which become inaccurate or unstable when information travels across multiple grid lengths in a single time step. For example, in the simple case described in Fig. 5.1 the time step must be chosen such that $\frac{u\Delta t}{\Delta x} < 1$ to avoid numerical instability. Versions of this limit, known as the Courant-Friedrichs–Levy (CFL) limit, exist for most explicit finite-difference schemes. In systems of equations that support propagating waves, as the primitive equations do, the relevant velocity in the CFL limit is typically the sum of the wave propagation speeds and the advective speed. Thus, the stability of explicit calculations is limited by the fastest wave modes in the system, which are often of little interest, for example, Lamb waves or deep gravity waves. Global models whose numerics are based on finite differences

("grid-point models") address this issue by introducing polar filters which are designed to suppress small-scale motions in the polar regions of the model.

A revolutionary innovation occurred in the late 1960s with the introduction of spectral techniques for solving the primitive equations [46]. Spectral models decompose the atmosphere into a finite sequence of spherical harmonic functions, rather than onto a grid of points. For example, the wind u is approximated by:

$$u(\lambda, \theta, z, t) = \sum_{n=0}^{N} \sum_{m=-n}^{n} U_n^m(z,t) Y_n^m(\lambda, \theta)$$

where λ is longitude and θ is latitude. The time evolution of the atmospheric flow is then represented as the time evolution of the amplitudes $U_n^m(z,t)$. Nonlinear advection terms arising in the primitive equations may be dealt with directly in spectral space, as interactions of spherical harmonics or in physical space with transformation of the tendencies back to spectral space [45].

The resolution of spectral models is determined by the truncation parameter N. The form of the finite sum used above is referred to as a triangular truncation. A model with $N = 799$ in this kind of decomposition is referred as a "T799" model. Lynch [2] gives a useful rule-of-thumb for estimating the spatial resolution Δ corresponding a particular value of N. He uses $\Delta \approx (2\pi a_e)/2\ N$ or $\Delta \approx (20{,}000\ km)/N$ where the circumference of the Earth $2\pi a_e$ has been approximated by 40,000 km.

Spectral techniques are not only highly accurate, but also nicely sidestep the pole problem faced by grid-point models formulated in terms of latitude and longitude on the sphere. Discretization into spherical harmonics produces no special difficulties at the poles.

A disadvantage of spectral schemes is that fields with strong variation across small-spatial scales, such as most trace gas concentrations (including water vapor), precipitation, or topography cannot be represented without introducing significant spurious nonlocal oscillations in these fields. This behavior, known as the Gibbs phenomenon is a simple consequence of attempting to represent highly localized features with global basis functions. The nature of these truncation errors is such that the amplitude of spurious oscillations decreases slowly with resolution. The presence of Gibbs oscillations can lead to serious problems in global simulations, such as the formation of negative trace gas concentrations.

Due to the difficulties in spectrally representing fields with intense spatial variability, grid-point models have not been abandoned. In addition, grid-point models can be made more efficient than spectral models at very high resolution. So, while most operational forecasting centers currently use some form of spectral dynamical core in their NWP models, this may change in the next decade. Current research is focused on developing grid-point or finite element approaches on nonstandard grids such as the icosahedral, that is, "bucky-ball" or "soccer-ball," grid to bypass the pole problem encountered in latitude-longitude discretizations (see section on "Future Directions") (Table 5.2).

Table 5.2 Parameterizations in Weather Forecasting models. The first column gives the usual designation used in the meteorological community. The second column summarizes the effects of the parameterization. The third column indicates the primitive equation forcing term in which tendencies from the parameterization appear

Parameterization	Effects	Included in
Deep convection	Transports heat, moisture and momentum vertically. Damps convergence	H_{phys}, $\mathbf{F}_{phys}$, $C_{i,phys}$
Orographic gravity wave drag	Decelerates flow over mountains	$\mathbf{F}_{phys}$
Planetary boundary layer (PBL) turbulence	Transports heat, moisture and momentum vertically	H_{phys}, $\mathbf{F}_{phys}$, $C_{i,phys}$
Radiation (Solar and IR)	Calculates heating due radiative flux convergence	H_{phys}
Diagnostic cloud	Estimates cloud cover and thickness	
Prognostic cloud	Calculates cloud condensate concentrations and estimates cloud optical properties	H_{phys}, $C_{i,phys}$

Parameterizations

Representation of physical processes such as radiation, turbulence, gravity wave drag, convection, and precipitation also became more sophisticated in NWP models as they evolved. The earliest successes in NWP using a filtered barotropic model did not even formally incorporate temperature as a prognostic variable. Today, NWP models may track several condensed water species, as well radiatively active trace gases such as ozone. It was the incorporation of radiative transfer schemes and simple moist convective adjustment schemes into NWP models in the 1960s [35] that led to the first climate models capable of self-consistently representing the basic feature of Earth's atmospheric general circulation.

Parameterization development for NWP models has followed that for climate models. The suite of parameterizations currently used in global NWP models is identical to that used for climate simulations. It is arguable whether most physics parameterizations exert an appreciable effect on short-term (1–3 day) forecasts. Deep convection and orographic wave drag parameterizations have been shown to exert a significant short-term effect [47–49]. At medium range (3 days to 2 weeks), physical parameterizations are thought to have an important effect on forecast skill (Bengtsson 2000). In addition climate biases resulting from deficient parameterizations can have a negative impact on data assimilation schemes (see section on "Data Assimilation Systems"). This can indirectly affect short-term forecasts by introducing errors in the initial conditions.

How Are NWP Models (Versus Climate Models) Evaluated?

Perhaps the most significant differences between global climate models and NWP models arise from the different jobs they are expected to perform. Ideally, a solver

for the primitive equations, coupled to set of physically realistic parameterizations of processes like convection, should perform both long-term and short-term simulations of the atmospheric flow with equal accuracy. However, this is not the case. Even when run at comparable resolutions, models developed for NWP and climate do not perform each other's tasks with comparable skill. The likely cause of this discordance is the process of model tuning. The need for "tuning" is widely recognized in both the NWP community and the climate modeling community as an inevitable consequence of using imperfect models [41]. The bulk of model tuning occurs in choosing empirical factors that regulate physical parameterizations. Some of this can be explained (or excused) as an attempt to represent unknown sub-grid distributions of quantities such as water vapor, temperature, or topographic roughness. Unfortunately, the process of selecting these empirical factors can be ad hoc, and parochial in character. Even if optimal tunings exist that combine high accuracy in short-term forecasting as well as unbiased climate simulations, they are unlikely to be found. Groups involved in developing climate models rarely have the computational resources to perform extensive testing of their models at high resolution in forecast mode, while NWP groups are typically under intense operational pressures, and have little time or incentive to examine their models in free-running climate simulations.

There is as yet no set of universally accepted metrics for climate models, although developments in this direction are taking place [50]. Metrics typically targeted by climate modelers include seasonal mean distributions of precipitation and seasonal mean planetary wave patterns. Other, functional, constraints exist for atmospheric models used in climate research. For example, when used in coupled climate simulations, that is, connected through boundary fluxes to ocean and land surface models, obtaining correct global budgets of energy and momentum in an atmospheric model is critical. Thus, intensive tuning of cloud parameterizations is usually conducted to ensure that seasonal and annual-mean radiation budgets at the top of the atmosphere are realistic, to minimize spurious long-term drift in extended simulations. Generally speaking, exact conservation of energy and momentum is a key concern in the design of atmospheric models for climate, while being of secondary importance in the design of NWP models.

On the other hand, operational NWP models are regularly subjected to a number of rigorous, and more-or-less universally accepted tests at each step in their development. Not surprisingly, these tests emphasize short-term simulation accuracy rather seasonal or annual-mean performance.

500 hPa Height Anomaly Correlation

At many centers including the European Center for Medium Range Weather Forecasting (ECMWF), the most important measure of global forecast model performance or skill is the 500 hPa height anomaly correlation. This measure is

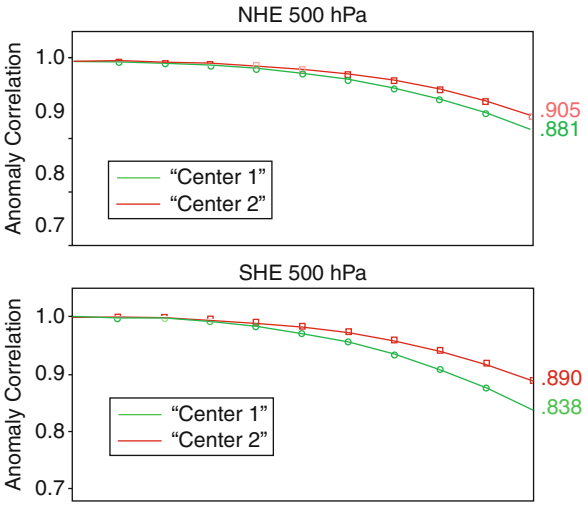

Fig. 5.2 Mean evolution of 500 hPa anomaly height correlation in two major global NWP models for the January through March

essentially the pattern correlation of two maps of geopotential height anomalies φ' interpolated to a pressure level of 500 hPa (corresponding to altitude close to 5 km). A height anomaly is defined the deviation in height from its average value along a latitude circle. One map is an analysis of height anomaly at 500 hPa $\phi'_{ana}(x,\ y,\ p_{500},\ t_a)$ (see section on "Initialization and Data Assimilation") and the second is a map of forecast height anomaly valid at the same time $\phi'_f(x,\ y,\ p_{500},\ t_a)$ where $t_a = t_i + \Delta t_f$. Here Δt_f is the forecast lead time and t_i is the initiation time. These two height fields are then used to form a correlation.

$$r_{500}(\Delta t_f) = \frac{\left\langle \phi'_f(t_i + \Delta t_f), \phi'_{ana} \right\rangle}{\sqrt{\left\langle \phi'_f, \phi'_f \right\rangle \left\langle \phi'_{ana}, \phi'_{ana} \right\rangle}}$$

where <> represents the spatial covariance over some region, typically the southern hemisphere or the northern hemisphere.

Figure 5.2 shows the average evolution of r_{500} in two major global forecast models for the period January 1 through March 31, 2009. The plots illustrate the state-of-the-art in NWP as of this writing. As expected the pattern correlations decrease with time, but remain quite high, above 0.8, out to a forecast lead of 5 days. Northern hemisphere correlations are higher in both systems, probably reflecting the higher density of in situ measurements available there. Many operational forecasting centers do not allow changes to their systems that degrade this measure of performance.

Although using r_{500} as *the* single measure of forecast accuracy may seem somewhat restrictive, it should noted that that the geopotential height φ at 500 hPa is an integrated measure of the temperature in a deep layer, form the surface to around 5,000 m. So, r_{500} is a concise summary of model performance in a horizontally extensive and deep atmospheric slab.

Skill Scores

The S1 skill score [51, 52] has been used since the 1950s by forecasters at the National Meteorological Center (NMC), and after 1995 the National Center for Environmental Prediction (NCEP), to evaluate forecast performance. An S1 score can be defined for any quantity. It is calculated:

$$S1(\chi) = 100 \times \frac{\int_A |\nabla(\chi_f - \chi_o)| dA}{\int_A \max(|\nabla\chi_f|,\ |\nabla\chi_o|) dA}$$

where χ_f is forecast χ and χ_o is the observed value for verification. $S1$ then is the ratio of the integrated absolute gradient in forecast error, normalized by the integrated absolute gradient of the quantity itself, where at each location the larger of the forecast or observed values is used. A value of $S1 = 0$ represents a perfect forecast. The quantity χ used to calculate $S1$ is typically sea-level pressure or geopotential height.

The $S1$ skill score was selected by NMC from many measures of forecast quality with guidance from practicing forecasters. Forecasters in 1950s noted that values of $S1$ around 20 corresponded to very good forecasts, while values of 70 or more represented nearly worthless forecasts. As a result, it became common practice to express "skill" as $2(70 - S1)$, so that now a very good forecast $S1 = 20$ has a skill score of 100, while useless forecasts have a skill score of 0 [52].

Equitable Threat Scores

Evaluation of precipitation forecasts is difficult for a number of reasons. Precipitation is a field with high variance and sharp boundaries. In many circumstances, the important forecast parameter is whether rain or precipitation (above a certain threshold) has occurred. Such categorical forecasts are evaluated using various methods based on matrices of possible outcomes, for example, **YY** – rain is forecast and occurs, **YN** – rain is forecast but does not occur, **NY** – rain is not forecast but occurs, and **NN** – rain is not forecast and does not occur. The most commonly used method is that of Equitable Threat Scores (ETS) [53] which attempts to account for the long-term statistical probability of each category.

Initialization and Data Assimilation

A moment's reflection shows that establishing initial conditions for a global model of the atmosphere is a nontrivial task. First of all, there may be instrumental errors

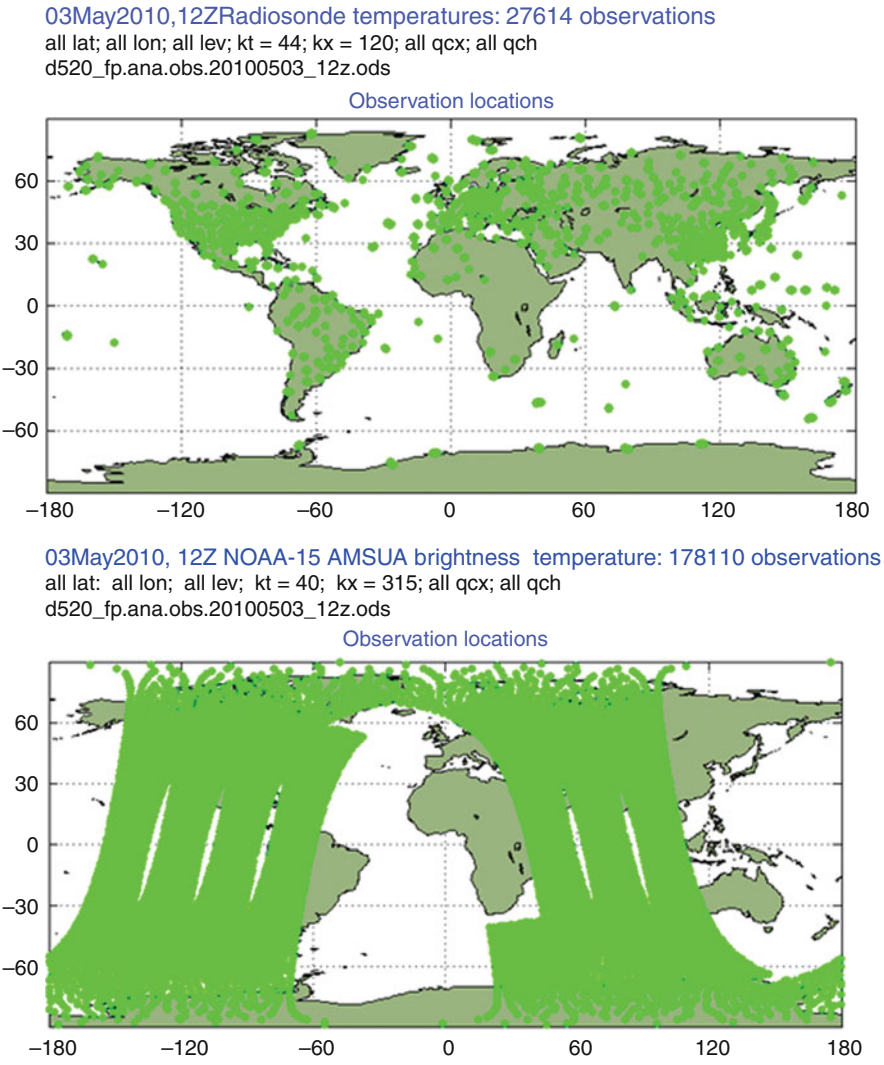

Fig. 5.3 Locations of radiosonde observations (*top*) and satellite temperature observations (*bottom*) for May 12, 2008 from NASA's GEOS-5 DAS

in the measurements of wind, temperature, humidity, or other quantities needed to specify the initial state of the atmosphere. While perhaps the most obvious problem, instrumental error may also be the least important problem faced in initialization. A more serious problem is hinted at in Fig. 5.3 which shows the current global distribution of radiosonde balloon launch sights. Radiosondes provide very accurate and reliable measurements of winds, temperatures, and humidities from the surface to around 10 km altitude. Launches are made by international agreement at either 0Z or 12Z ("Z" refers to Greenwich mean time) or at both times, depending

on the station. However, as the figure shows, radiosonde launch sites are distributed in a completely unstructured way across the globe. High concentrations occur in the developed world, with sparse or no coverage over oceans and over less-developed land areas. Even in the developed world the location of sites is determined by human factors – and is more-or-less spatially random. Numerical models of the atmosphere, both spectral and grid point, require a spatially structured set of numbers to begin their integrations. Satellite data presents similar challenges. While it is structured – along orbital tracks – the structure does not conform to the needs of NWP models. In addition, satellite data is asynchronous, that is, sampling occurs continuously as the satellite travels, not at a specified time as with radiosonde data.

Thus a major challenge faced in NWP is to derive a complete model state on a structured set of points at a single instant in time, from data that may be neither spatially structured nor representative of a single point in time. Naive interpolation in space and/or time is inadequate. The model state derived from the data must not only cover the globe, it must do so while also satisfying a number of other dynamical and physical constraints.

Fluid flows, and vector fields in general, can be decomposed into a sum of divergent ($\nabla \cdot \mathbf{u_1} \neq 0$) and nondivergent ($\nabla \cdot \mathbf{u_2} = 0$) components. Generally speaking, the atmospheric motions of most significance in 1–5 day forecasts are characterized by "small" horizontal convergence and divergence in a relative sense. In these flows, two or three of the terms in the momentum equation form a dominant steady-state balance that describes the flow to first-order. These balanced flows are *almost* nondivergent. However, their time evolution can be profoundly affected by the small divergent component. The earliest and most basic balance identified by meteorologists is the so-called geostrophic balance, described below. The subtleties of the divergent wind field in geostrophically balanced flow are what doomed L. F. Richardson's pioneering NWP experiment.

Geostrophically Balanced Flow

The origin of geostrophic balance is most easily seen by performing a scale analysis of the momentum equation in the primitive equation system. Scale analysis is a common procedure in fluid mechanics to systematically identify the most important terms in the complicated equations describing fluid flow [4]. It begins by identifying scales of motion for the phenomenon of interest. For midlatitude weather systems, especially after considering the spacing and resolution of radiosonde and satellite data, a reasonable choice of spatial scale L is around 1,000 km. Other reasonable choices of scales are for horizontal wind $U \sim 10\ \mathrm{ms}^{-1}$, and for pressure disturbance $P \sim 10$ hPa or 1,000 Pa. These scales along with local apparent rotation rate f with values $\sim 10^{-4}\ \mathrm{s}^{-1}$ in midlatitudes are used to estimate the sizes of the terms in the equation. For example, $\frac{d}{dt}V$ will be $\sim U^2/L$ where the horizontal advective time scale has been

used as the relevant time scale. It is easy to see that the ratio of this term to the Coriolis term $f\mathbf{k} \times V$ will scale as U/fL, which is a key nondimensional parameter in dynamic meteorology known as the Rossby number or Ro. For the scales of motion typical for midlatitude systems, Ro is close to 0.1. So the advective term is likely to small compared to the Coriolis term and also, it turns out, compared to the pressure gradient.

Thus, the "leading order" balance in midlatitude systems is left as:

$$f\mathrm{k} \times V = -\alpha \nabla_z p$$

where we have used height as the vertical coordinate. Equivalent expressions exist for other vertical coordinates. In component form this balance is written as:

$$-fv = -\alpha \partial_x p\,;\; fu = -\alpha \partial_y p$$

This balance is the dominant feature of midlatitude flow. It is also responsible for one of the most counterintuitive aspects of weather maps in midlatitudes – that the wind blows along pressure contours rather than from high pressure to low pressure. It is also the reason air flows in a counterclockwise sense around low-pressure centers in the northern hemisphere. A perplexing aspect of this balance is that it is a steady-state relation. In other words, the largest forces in the system give no information about its time evolution.

It is easy to see that this leading-order geostrophic flow is horizontally nondivergent. However, spurious divergent flow features can easily appear when constructing initial conditions from observations of horizontal. An idea of the difficulty of this challenge can be obtained by considering the following argument. The relative vorticity of the horizontal wind is determined from:

$$\zeta = \partial_x v - \partial_y u$$

and, further scale analysis of the equations of motion in midlatitudes (see [45]) shows that the ratio $\nabla \cdot V$ to ζ will typically be close to Ro or ~ 0.1. The individual horizontal derivative terms in the expressions for vorticity and divergence are of the same order. The small relative magnitude of $\nabla \cdot V$ is only possible through near cancelation of its much larger component terms. It is not trivial to maintain this cancelation during the data assimilation process. Errors in the divergence can have large effects on surface pressure tendencies since

$$\partial_t p_s \sim p_s \nabla \cdot V.$$

More complete and correct balance relationships than geostrophic balance can be derived [54]. Balanced initial conditions have been sought in a number of ways during the history of NWP. The most successful of these was perhaps nonlinear normal mode initialization introduced in the 1970s [55–57]. In this technique, fast and slow normal modes of the nonlinear equations of motion are found through an iterative procedure.

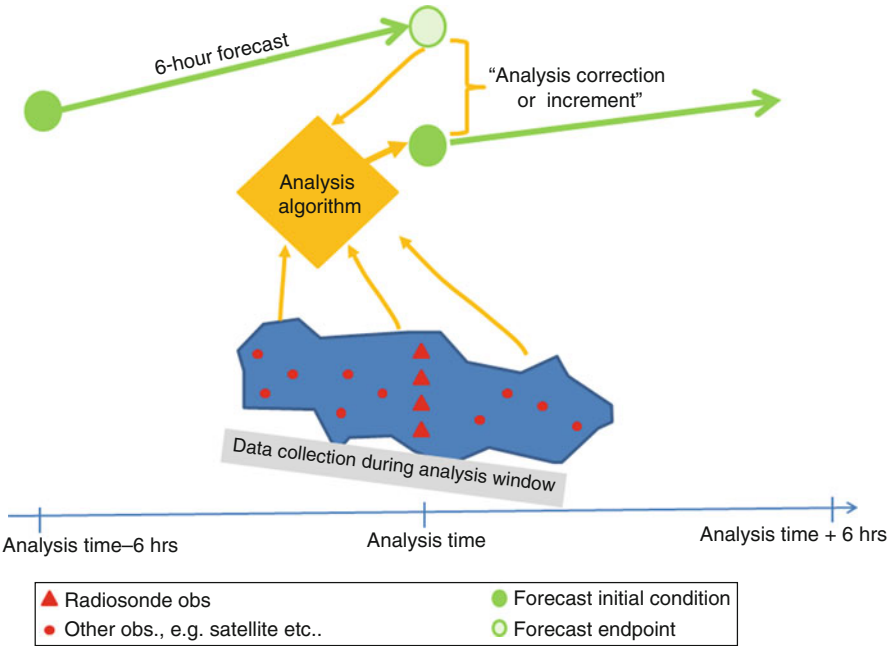

Fig. 5.4 Schematic diagram of 3D-var analysis

Data Assimilation Systems

Modern operational centers handle the problem of initializing their forecasts by using a data assimilation system (DAS). A central feature of a DAS is the forecast model itself (or a linearized version thereof). Analyses at operational forecasting centers are typically performed four times daily at 00Z, 06Z, 12Z, and 18Z. The analysis procedure combines measurements with a short model forecast, typically 6 h initialized with the previous analysis. This forecast is often referred to as the "first guess" or "background." The job of the analysis algorithm, denoted by the yellow diamond in Fig. 5.4, is to blend the myriad sources of data, which includes radiosonde observations satellite measurements, pilot reports, surface station reports, ship buoy measurements, and more, with the forecast to produce an optimal estimate of the state of the atmosphere on the model grid. The process illustrated in Fig. 5.4 depicts a "3D-Var" system. In 3D-Var, data gathered within an analysis time window, typically 3 h before and after the standard analysis times, is assumed to be synchronous. The analysis then consists of an optimal blending of measurements and forecast background in space.

This optimal blending can be expressed as a "cost function minimization." The cost function is written in matrix form [2, 54, 58]:

$$J(\mathrm{x}) = (\mathrm{x} - \mathrm{x}_b)T\ \mathrm{B}^{-1}(\mathrm{x} - \mathrm{x}_b) + [\mathrm{y} - H(\mathrm{x})]^T\ \mathrm{R}^{-1}[\mathrm{y} - H(\mathrm{x})] + J_b(\mathrm{x})$$

where **x** is a model "state vector," that is V, T, q and possibly other analyzed species on the model's numerical grid (or spectral decomposition). The quantity $\mathbf{x}_b$ is the model state from a forecast, that is, the first guess or background, and the matrix **B** is the background, or forecast, error covariance matrix. This matrix is a key piece of the analysis algorithm, and is estimated by examining differences between forecasts radiosonde observations [59] or more recently by calculating the covariance of different short forecasts, for example, 24 h and 48 h, valid at the same time [60, 61].

The second term in the cost function contains the observation error covariance matrix **R**, the observation vector **y** and a vector $H(\mathbf{x})$ which is the result of the "observation operator" H acting on the model state **x**. In the case of an observation taken by a thermometer placed at a model grid-point, the observation operator would simply select the appropriate element of **x**. However, in the case of remote satellite observations, which directly measure radiances (photons) from the atmosphere, H could represent a complex radiative transfer calculation using for example T and q from the model state to estimate the radiance measured by a particular instrument. The approach of transforming model quantities into a form that is directly comparable with observations, sometimes referred to as "radiance assimilation," led to dramatic increases in the positive impact of satellite measurements on forecasting [62].

The third term in the cost function represents balance constraints on the flow, such as those discussed in the section on "Geostrophically Balanced Flows". Inclusion of such a term at NCEP has eliminated the need for a separate initialization procedure for forecasts [60].

The task of the analysis algorithm is to find the model state $\mathbf{x}_a$ that minimizes the cost function $J(\mathbf{x})$. For more details on how this solution is actually accomplished the reader is referred to discussion in Chap. 5 of Kalnay (2003) [54]. 3D-var as described here is used by NCEP as well as in slightly modified version by NASA's Global Modeling and Assimilation Office (GMAO) in their GEOS-5 DAS [63]. A somewhat different approach known as 4D-Var is used at ECMWF. This approach takes into account the possibly asynchronous nature of data when formulating the cost function. For more details, see the discussion in Kalnay (2003).

Ensemble Forecasting

The early thinking of researchers in NWP was that the central problem of forecast initialization was to correctly filter out rapid divergent motions, and, that once this was accomplished no fundamental limits on atmospheric predictability existed. A series of

seminal papers by Edward N. Lorenz proved this to be incorrect [64–66]. Lorenz showed that simple analogs to atmospheric equations of motion possess a sensitive dependence to initial conditions. In other words, small differences in even well-balanced initial conditions will cause forecasts to become uncorrelated after a finite time.

Modern operational forecasting centers typically perform ensembles of many runs with slightly different initial conditions, as well as a single higher-resolution "deterministic" run to produce forecasts for a given time [54, 67]. The generation of ensemble members is a nontrivial task. Ideally, the members of the ensemble should vary in special directions in phase space that are related to the most rapidly growing instabilities in the flow [54, 68].

Future Directions

Weather forecasts have improved demonstrably during the 50 year history of NWP. This is illustrated in Fig. 5.5, which shows the evolution of r_{500} at 3, 5, and 7 days over the last 30 years in the ECMWF system [69]. Part of the improvement is traceable to the explosion in the amount of satellite data over the last 30 years. However, a large part of the improvement in skill is due to improvements in the forecast and analysis "system," such as increased forecast model resolution, improved analysis algorithms etc. This is nicely demonstrated in the bottom panel of Fig. 5.5, which shows the evolution of skill in retrospective forecasts, using the *current* ECMWF system on the historical data base. The skill of retrospective forecasts is significantly higher, indicating that the improved forecast and analysis system makes a significant, perhaps the dominant, contribution to the overall increase in skill seen in the last 30 years. One aspect of improvement that is clearly due to improved data sources (satellites) is the convergence of skill in southern and northern hemispheres.

Scalable Dynamical Cores

As computing power increases NWP model resolution also continues to increase. In the last several years, the increase in computer power has appeared primarily in the form of massively parallel machines with larger and larger numbers of processors, rather than in the form of faster individual processors. This means that "time-to-solution" has not decreased dramatically in recent years, but the size of feasible calculations has increased dramatically. This has stimulated the development of scalable models. Scalability means that model speed increases more-or-less linearly with the number of processors used. A trivial example of perfectly scalable problem is the addition of 1,000 pairs of numbers a + b = c. If one processor is available then the calculation will take 1,000 CPU time units. If 1,000 processors are available the

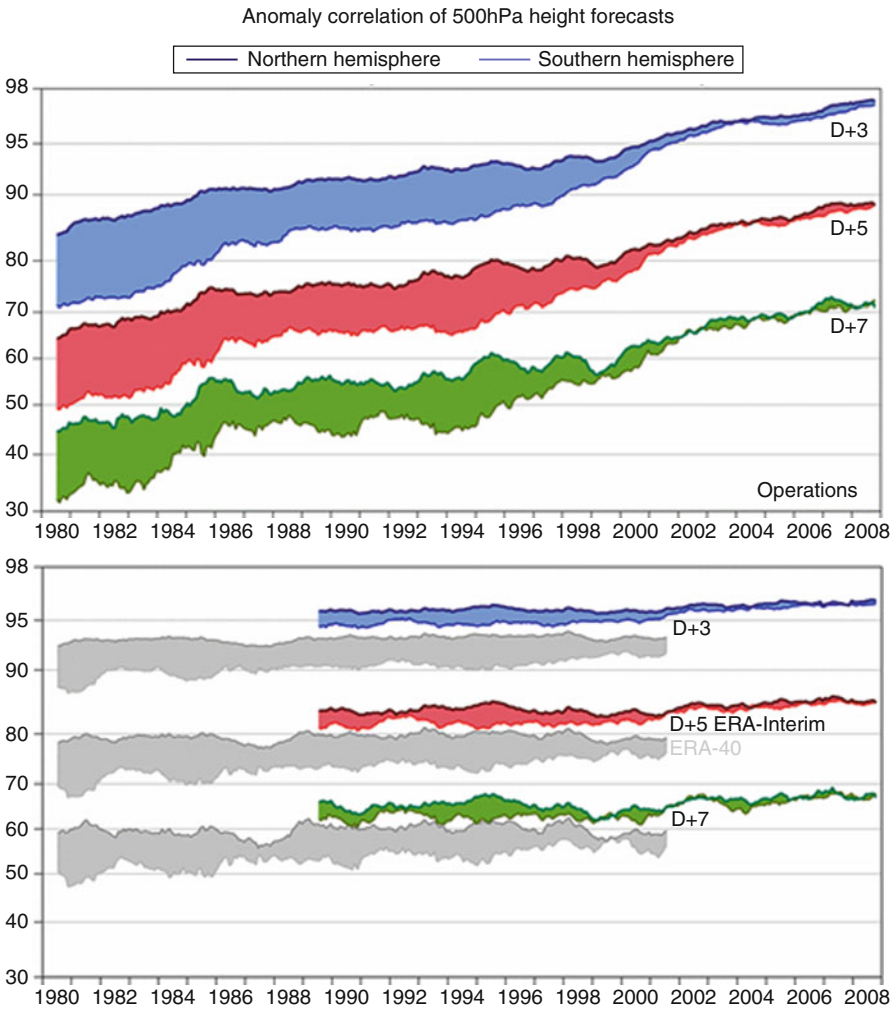

Fig. 5.5 Evolution of forecast skill at ECMWF, adapted and extended from the study of Simmons and Hollingsworth (2002). The *top panel* shows a history of r_{500} at 3, 5, and 7 days from the ECMWF operational forecast beginning in 1980. The *colored* and *shaded areas* are bounded by southern hemisphere skill below and northern hemisphere skill above. The *lower panel* shows retrospective forecasts produced using two versions of current ECMWF analysis and forecast systems. In these cases, the "system" is fixed in time, while data inputs evolve in actual historical fashion

entire calculation can take place in 1 CPU time unit. However, communication between processors also costs time. In any real numerical model of the atmosphere processors eventually need information residing in other processors. This prevents numerical models of the atmosphere from scaling perfectly.

The amount of cross-processor communication required can vary widely depending on model design. Ideally decomposition will maximize the ratio of

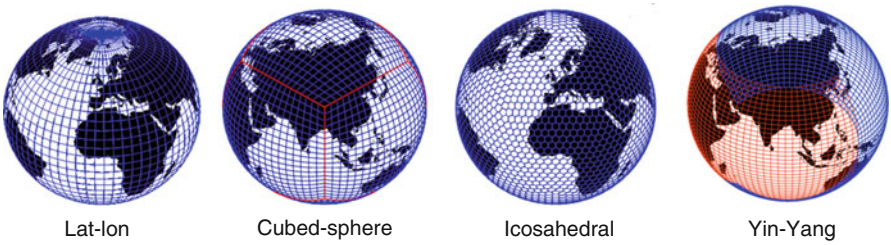

Fig. 5.6 The standard latitude-longitude "lat-lon" grid (*leftmost globe*) compared with newer, non-traditional grids for global atmospheric models

area to perimeter in computational subdomains to minimize the need for cross-processor communication. The scalability of grid-point models on latitude-longitude grids is severely hampered by the need to apply polar filters to overcome numerical instabilities that arise due to the convergence of longitude lines at both poles. These filters typically require knowledge of atmospheric fields all the way around latitude circles. Thus, modelers must either decompose the globe into thin computational domains circling the globe, which will lead to large communication requirements in the north–south direction, or they must pay the cost of frequent "gathers" to obtain the necessary inputs for polar filters. Transforms in spectral models likewise require knowledge of fields around latitude circles.

Recent efforts in numerical techniques for global atmospheric models have focused on the development of grid-point or finite element models on nonstandard grids [70–73]. Several examples of such grids are shown in Fig. 5.6. These grids have fairly uniform grid cell sizes over the entire globe. Polar filters are therefore not required.

Nonhydrostatic Dynamics

Once horizontal resolution becomes much finer than 10 km, nonhydrostatic effects must be taken into account. This will require models based on a different set of equations. One option is to simply use the full Euler or Navier Stokes equations [39, 74] and pay the costs associated with the short time-steps required by the presence of acoustic waves. Another approach is to use an inelastic equations system [75], but this requires solution of an elliptic equation which is an intrinsically nonlocal procedure and again raises cross-processor communication costs.

Seamless Models for Climate and Weather

Modern global NWP and climate models are essentially the same. Both use the same set of dynamical equations (see section on "Primitive Equations"). Both also

use the same set of physical parameterization schemes (see section on "Parameterization"). In practice, differences do exist between global models of the atmosphere intended for climate simulation and those intended for forecasting. Operational global NWP models have typically used resolutions that are a factor of 8–16 times higher than those used in long climate simulations. Other differences arise, more-or-less unintentionally, in the tuning process as a consequence of the different metrics used in the evaluation of NWP and climate models (see section on How are NWP models (versus climate models) evaluated?).

Climate researchers understand that atmospheric phenomena such as squall lines and tropical cyclones may play a role in establishing climate on both regional and global scales. Such "mesoscale" features are not resolved in climate models with resolutions of 100 km or coarser. However, the continued increase in computer power, and the recent emphasis on massively parallel architecture, will allow decadal or even century-long simulations at resolutions close to 10 km in the near future. At these resolutions, mesoscale circulations should be well represented. These resolutions will also present novel challenges to the sub-grid parameterizations used in climate models, as assumptions about scale-separation and statistical equilibrium become questionable.

Bibliography

1. Tribbia J, Anthes R (1987) Scientific basis of modern weather prediction. Science 237:493–499
2. Lynch P (2006) The emergence of numerical weather prediction: Richardson's dream. Cambridge University Press, Cambridge, MA
3. Richardson L (1922) Weather prediction by numerical process. Cambridge University Press, Cambridge
4. Gill A (1982) Atmosphere–ocean dynamics. Academic, London
5. Simpson J (1994) Sea breeze and local winds. Cambridge University Press, New York
6. Lau K, Li M (1984) The monsoon of East Asia and its global associations_survey. Bull Amer Meteor Soc 65:114–125
7. Webster P, Tomas R (1998) Monsoons- processes, predictability, and the prospects for prediction. J Geophys Res 103(C7):14451–14510
8. Douglas M, Maddox R, Howard K, Reyes S (1993) The Mexican monsoon. J Clim 6(8):1665–1677
9. Koch S, Handley C (1997) Operational forecasting and detection of mesoscale gravity waves. Weather Forecast 12(2)
10. Moncrieff M, Liu C (1999) Convection initiation by density currents: role of convergence, shear, and dynamical organization. Mon Weather Rev 127(10):2455–2464
11. Lac C, Lafore J, Redelsperger J (2002) Role of gravity waves in triggering deep convection during TOGA COARE. J Atmos Sci 59(8)
12. Houze R Jr (2004) Mesoscale convective systems. Rev Geophys 42. doi:10.1029/2004RG000150
13. Grabowski W, Moncrieff M (2006) Large-scale organization of tropical convection in two-dimensional explicit numerical simulations. Q J Roy Meteor Soc 127(572):445–468
14. Smith R (1979) The influence of mountains on the atmosphere. Adv Geophys 21:87–230

15. Longuet-Higgins M (1964) Planetary waves on a rotating sphere. Proc R Soc Lond A Math Phys Sci 279(1379):446–473
16. Andrews D, McIntyre M (1976) Planetary waves in horizontal and vertical shear: the generalized Eliassen-palm relation and the mean zonal acceleration. J Atmos Sci 33:2031–2048
17. Hoskins B, Ambrizzi T (1993) Rossby wave propagation on a realistic longitudinally varying flow. J Atmos Sci 50:1661–1671
18. Charney J (1947) The dynamics of long waves in a baroclinic westerly current. J Meteor 4(5):135–162
19. Eady E (1949) Long waves and cyclone waves. Tellus 1(3):33–52
20. Kiladis G, Wheeler M, Haertel P, Straub K, Roundy P (2009) Convectively coupled equatorial waves. Rev Geophys 47. doi:10.1029/2008RG000266
21. Burpee R (1972) The origin and structure of easterly waves in the lower troposphere of North Africa. J Atmos Sci 29(1):77–90
22. Landsea C et al (1993) A climatology of intense (or major) Atlantic hurricanes. Mon Weather Rev 121(6):1703–1713
23. Pytharoulis I, Thorncroft C (1999) The low-level structure of African easterly waves in 1995. Mon Weather Rev 127(10)
24. Thorncroft C, Hodges K (2001) African easterly wave variability and its relationship to Atlantic tropical cyclone activity. J Clim 14(6):1166–1179
25. Madden R, Julian P (1994) Observations of the 40–50-day tropical oscillation: a review. Mon Weather Rev 122(5):814–837
26. Zhang C (2005) Madden-Julian oscillation. Rev Geophys 43(2). doi:10.1029/2004RG000158
27. Liebmann B, Hendon H, Glick J (1994) The relationship between tropical cyclones of the western Pacific and Indian Oceans and the Madden–Julian oscillation. J Meteor Soc Japan 72(41):1–412
28. Maloney E, Hartmann D (2000) Modulation of hurricane activity in the Gulf of Mexico by the Madden-Julian oscillation. Science 287(5460):2002
29. Maloney E, Hartmann D (2000) Modulation of eastern North Pacific hurricanes by the Madden-Julian oscillation. J Clim 13(9)
30. Elsner J, Jagger T, Niu X et al (2000) Changes in the rates of North Atlantic major hurricane activity during the 20th century. Geophys Res Lett 27(12):1743–1746
31. Hall J, Matthews A, Karoly D (2001) The modulation of tropical cyclone activity in the Australian region by the Madden–Julian oscillation. Mon Weather Rev 129:12
32. Bond N, Vecchi G (2003) The influence of the Madden–Julian oscillation on precipitation in Oregon and Washington. Weather Forecast 18(4):600–613
33. Jones C, Waliser D, Lau K, Stern W (2004) The Madden–Julian oscillation and its impact on northern hemisphere weather predictability. Mon Weather Rev 132(6)
34. Waliser DE, Lau KM, Stern W, Jones C (2003) Potential predictability of the Madden–Julian oscillation. Bull Amer Meteor Soc 84:33–50
35. Manabe S, Smagorinsky J, Strickler R (1965) Simulated climatology of a general circulation model with a hydrologic cycle. Mon Weather Rev 93(12):769–798
36. Namias J (1980) The early influence of the Bergen School on synoptic meteorology in the United States. Pure App Geophys 119(3):491–500
37. Grenas S (2005) Vilhelm Bjerknes' vision for scientific weather prediction. In: The Nordic seas: an integrated perspective: oceanography, climatology, biogeochemistry, and modeling. American Geophysical Union, Washington, DC, p 357
38. Hinkelmann K (1951) Der Mechanismus des meteorologischen Lärmes. Tellus 3:285–296
39. Laprise R (1992) The Euler equations of motion with hydrostatic pressure as an independent variable. Mon Weather Rev 120(1):197–207
40. Shuman F, Hovermale J (1968) An operational six-layer primitive equation model. J Appl Meteor 7(4):525–547

41. Bengtsson L (2001) The development of medium range forecasts. In: 50th anniversary of numerical weather prediction, commemorative symposium, Potsdam
42. Kasahara A (2000) On the origin of cumulus parameterization for numerical prediction models. Gen Circ Model Dev 70:199–224
43. Tiedtke M (1993) Representation of clouds in large-scale models. Mon Weather Rev 121:3040–3061
44. Del Genio A, Yao M, Kovari W, Lo K (1996) A prognostic cloud water parameterization for global climate models. J Clim 9:270–304
45. Haltiner G, Williams R (1983) Numerical prediction and dynamic meteorology, 2nd edn. Wiley, New York
46. Leith C (1965) Numerical simulation of the earth's atmosphere. In: Methods in computational physics, vol 4. Academic, New York
47. Webster S, Brown A, Cameron D, Jones C (2006) Improvements to the representation of orography in the Met Office Unified Model. Q J Roy Meteor Soc 129(591):1989–2010
48. Clark A, Gallus W Jr, Xue M, Kong F (2009) A comparison of precipitation forecast skill between small convection-allowing and large convection-parameterizing ensembles. Weather Forecast 24(4):1121–1140
49. Bhanu Kumar O, Ramalingeswara Rao S, Muni Krishna K (2009) Role of cumulus parameterization schemes in simulating heavy rainfall episodes off the coast of Maharashtra state during 28 June–4 July 2007. Meteorol Atmos Phys 105(3):167–179
50. Gleckler P, Taylor K, Doutriaux C (2008) Performance metrics for climate models. J Geophys Res 113:D06104
51. Teweles S, Wobus H (1954) Verification of prognostic charts. Bull Amer Meteor Soc 35:455–463
52. Shuman F (1989) History of numerical weather prediction at the National Meteorological Center. Weather Forecast 4:286–296
53. Gandin L, Murphy A (1992) Equitable skill scores for categorical forecasts. Mon Weather Rev 120:361–370
54. Kalnay E (2003) Atmospheric modeling, data assimilation, and predictability. Cambridge University Press, Cambridge, MA
55. Machenhauer B (1977) On the dynamics of gravity oscillations in a shallow water model, with applications to normal mode initialization. Beitr Phys Atmos 50:253–271
56. Baer F, Tribbia J (1977) On complete filtering of gravity modes through nonlinear initialization. Mon Weather Rev 105(12):1536–1539
57. Tribbia J (1984) A simple scheme for high-order nonlinear normal mode initialization. Mon Weather Rev 112:278–284
58. Daley R (1993) Atmospheric data analysis. Cambridge University Press, New York
59. Thiebaux HJ, Pedder MA (1987) Spatial objective analysis with applications in atmospheric science. Academic, London/Orlando, p 308
60. Parrish D, Derber J (1992) The National Meteorological Center's spectral statistical-interpolation analysis system. Mon Weather Rev 120(8):1747–1763
61. Buehner M, Gauthier P, Liu Z (2005) Evaluation of new estimates of background-and observation-error covariances for variational assimilation. Q J Roy Meteor Soc 131(613):3373–3384
62. Derber J, Wu W (1998) The use of TOVS cloud-cleared radiances in the NCEP SSI analysis system. Mon Weather Rev 126(8):2287–2299
63. Rienecker M, Suarez M, Todling R, Bacmeister J, Takacs L, Liu H, Gu W, Sienkiewicz M, Koster R, Gelaro R et al (2008) The GEOS-5 data assimilation system-documentation of versions 5.0.1, 5.1.0. NASA Technical Memorandum, NASA/TM-2007, 104606
64. Lorenz E (1965) A study of the predictability of a 28-variable atmospheric model. Tellus 17(3):321–333
65. Lorenz E (1969) The predictability of a flow which possesses many scales of motion. Tellus 21(3):289–307

66. Lorenz E (1969) Atmospheric predictability as revealed by naturally occurring analogues. J Atmos Sci 26(4):636–646
67. Lewis J (2005) Roots of ensemble forecasting. Mon Weather Rev 133(7):1865–1885
68. Toth Z, Kalnay E (1993) Ensemble forecasting at NMC: the generation of perturbations. Bull Amer Meteor Soc 74:2317–2330
69. Simmons A, Hollingsworth A (2002) Some aspects of the improvement in skill of numerical weather prediction. Q J Roy Meteor Soc 128(580):647–678
70. Ringler T, Heikes R, Randall D (2000) Modeling the atmospheric general circulation using a spherical geodesic grid: a new class of dynamical cores. Mon Weather Rev 128(7):2471–2490
71. Skamarock W, Klemp J, Ringler T, Thuburn J (2008) A hexagonal C-grid atmospheric core formulation for multiscale simulation on the sphere. AGU fall meeting abstracts, San Francisco, CA, p 01
72. Putman W, Lin S (2009) A finite-volume dynamical core on the cubed-sphere grid. Astron Soc Pac Conf Ser 406:268
73. Taylor M, Fournier A (2010) A compatible and conservative spectral element method on unstructured grids. J Comput Phys 229:5879–5895
74. Klemp J, Skamarock W, Dudhia J (2007) Conservative split-explicit time integration methods for the compressible nonhydrostatic equations. Mon Weather Rev 135(8):2897–2913
75. Grabowski W, Smolarkiewicz P (2002) A multiscale anelastic model for meteorological research. Mon Weather Rev 130(4)